This is the accepted manuscript made available via CHORUS. The article has been published as:

Half-Heusler Semiconductors as Piezoelectrics

Anindya Roy, Joseph W. Bennett, Karin M. Rabe, and David Vanderbilt

Phys. Rev. Lett. **109**, 037602 — Published 18 July 2012

DOI: 10.1103/PhysRevLett.109.037602

Half-Heusler semiconductors as piezoelectrics

Anindya Roy,* Joseph W. Bennett,* Karin M. Rabe, and David Vanderbilt
Department of Physics and Astronomy
Rutgers University, Piscataway, NJ 08854

We use a first-principles rational-design approach to demonstrate the potential of semiconducting half-Heusler compounds as a previously-unrecognized class of piezoelectric materials. We perform a high-throughput scan of a large number of compounds, testing for insulating character and calculating structural, dielectric, and piezoelectric properties. Our results provide guidance for the experimental realization and characterization of high-performance materials in this class that may be suitable for practical applications.

PACS numbers: 77.65.Bn, 81.05.Zx, 77.84.-s

One of the central challenges in materials science is the design of multifunctional materials, in which large responses are produced by applied fields and stresses. A rapidly developing paradigm for the rational design of such materials is based on the first-principles study of a large family of materials. First principles calculations of structure and properties are used to explore the microscopic origins of the functional properties of interest, and this information is used to guide the computational screening of many compounds, in both equilibrium and metastable structures, to identify promising candidate systems. A prototypical example is the optimization of piezoelectricity in perovskite oxides. The piezoelectric coefficients, describing the strain induced by an applied electric field or equivalently a voltage difference induced by applied stress, can be readily computed from first principles [1, 2]. Screening of a large number of systems has identified candidate materials for high-performance actuator and sensor applications [3, 4].

Another large family of materials is that of the ABC half-Heusler compounds (MgAgAs structure type, also called semi-Heusler or Juza-Nowotny compounds [5]), with almost 150 distinct compounds reported in the *Inorganic Crystal Structural Database* (ICSD) [6]. The half-Heusler structure, shown in Fig. 1, has $F\bar{4}3m$ symmetry and can be viewed as a rocksalt lattice formed from two of the three constituent atoms (at Wyckoff positions 4a and 4b), with the third atom filling half of the tetrahedral interstitial sites (either Wyckoff position 4c or 4d); it is related to the A_2BC Heusler structure by removal of one of the A sublattices, and can alternatively be viewed as a stuffed AC or BC zincblende structure [7].

Following an initial wave of interest stimulated by the observation of half-metallic ferromagnetic behavior in half-Heusler compounds [8], there has been a resurgence of interest in these compounds as materials that can display topological properties [9, 10] or be tailored for uses as diverse as components in spintronic devices [11] and high-performance thermoelectrics [12–14]. The semiconducting half-Heusler compounds are of particular interest [15, 16]. As insulators, these can exhibit functional properties associated with electric polarization, but these properties have received very little attention. In fact, while the $F\bar{4}3m$ space group of the half-Heusler structure allows a nonzero piezoelectric response, no measurements of piezoelectricity in these systems have yet been reported in the literature.

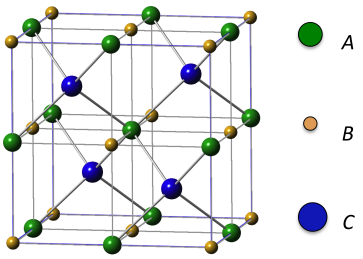

FIG. 1. (Color online) The ABC half-Heusler structure: A (green) and B (orange) are arranged in a rocksalt lattice, with the tetrahedral coordination of C (blue) by A shown.

In this paper, we use first-principles methods to predict the piezoelectric response and related properties of half-Heusler compounds. We present these predictions first for compounds already reported in the half-Heusler structure, and then perform a high-throughput analysis of a much larger set of candidate combinations, identifying high-performance compounds for practical application. We find that half-Heusler compounds exhibit a wide range of shear piezoelectric constants; the highest values (found for as-yet hypothetical compounds) are well above $d_{14} = 200\,\mathrm{pC/N}$. This compares well to known piezoelectric oxides such as PZT with $d_{33} \approx 300\,\mathrm{pC/N}$ and ZnO with $d_{33} \approx 10\,\mathrm{pC/N}$. In addition, the diversity of possible combinations could allow for other desirable functional properties to couple to piezoelectricity. Through targeted synthesis, which might include compositional substitution, epitaxial growth or artificial structuring, half-Heusler compounds could thus be developed as a valuable class of piezoelectric materials, much like the perovskite oxides.

First-principles calculations are performed with the ABINIT package [17–19] using the local density approxi-

mation (LDA) and an 8×8×8 Monkhorst-Pack sampling of the fcc Brillouin zone [20]. Optimized [21] designed non-local [22] norm-conserving pseudopotentials, generated using the OPIUM code [23], are employed, with a plane-wave cutoff of 25 Ha.

For the high-throughput search, we consider combinations of three distinct elements ABC. We limit the search to combinations with a total of 8 s and p valence electrons, since we expect this to improve the likelihood of band gap formation [7]. We also require that there be at least one and at most two p-block elements among the three constituents, with the remainder coming from the s and/or d blocks of the periodic table. We use Roman numerals to denote the valences of the constituent elements (including d electrons) to classify the combinations into families with 8 valence electrons (I-I-VI, I-II-V, I-III-IV, II-II-IV, and II-III-III), 18 valence electrons (XI-I-VI, XI-II-V, XI-III-IV, I-XII-V, II-XII-IV, III-XII-III, X-II-VI, X-III-V, and X-IV-IV), or 28 valence electrons (X-XII-VI, XI-XI-VI, XI-XII-V and XII-XII-IV). Among these families, we consider members constructed from the selections I=(Li, Na, K), II=(Be, Mg, Ca, Sr, Ba), III=(B, Al, Ga, In, Sc, Y), IV=(C, Si, Ge, Sn, Pb, Ti, Zr, Hf), V=(N, P, As, Sb, Bi), VI=(O, S, Se, Te), X=(Ni, Pd, Pt), XI=(Cu, Ag, Au), and XII=(Zn, Cd). This generates a total of 987 candidate combinations to be searched.

We first consider the 38 combinations in our search set that have been experimentally reported in the ICSD in the half-Heusler structure. For each combination, we optimize the lattice constant for each of the three structural variants $\underline{A}BC$, $A\underline{B}C$, and $AB\underline{C}$, where the underscore indicates the unique element that is tetrahedrally coordinated by the other two elements. First-principles results show that 27 of them, listed in Table I, are insulating. The predicted lowest-energy structural variant is indicated in the first column. We find that for the five compounds (LiZnAs, AuScSn, NiScSb, PdScSb and PtYSb) for which a refined structure, including R value and temperature factors, is available in ICSD, our prediction agrees with the experimentally observed variant. Most of the computed equilibrium lattice constants given in Table I are in excellent agreement with experiment. There are a few exceptions, LiInSi, LiGaSi and LiZnP, for which the DFT values, confirmed by independent all-electron calculations, differ significantly from the experimentally measured values; further experimental investigation of these cases is warranted. The computed gaps range from 0.07 eV for AuYPb and LiInSi to 1.55 eV for LiMgAs; measured values are expected to be higher given the well-known tendency of DFT to underestimate band gaps.

For each compound, we perform a linear-response calculation using density-functional perturbation theory (DFPT) [24], as implemented in ABINIT, to compute the electronic dielectric constant ϵ_∞, dynamical charges and zone-center phonon frequencies and eigenvectors, from which we obtain the zero-stress static dielectric constant ϵ_0 [25], reported in Table I. Calculations of the strain response [1, 26] yield the C_{44} elastic constant and e_{14} piezoelectric coefficient, also reported in Table I. These results determine $d_{14} = e_{14}/C_{44}$ and the electromechanical coupling coefficient k_{14}, the conventional figure of merit for piezoelectric performance, as $k_{14} = |e_{14}|/\sqrt{C_{44}\epsilon_{\rm fs}\epsilon_0}$, where $\epsilon_{\rm fs}$ is the permittivity of free space [1]. We note that C_{44}, especially when it is very small, is difficult to calculate precisely, the more so as it is also sensitive to the value of the lattice parameter. There is a corresponding uncertainty in d_{14}. However, k_{14} is less affected as it depends on C_{44} only as $1/\sqrt{C_{44}}$. Also, we note that ϵ_∞ and therefore ϵ_0 is generally overestimated in DFT, and $k_{14} \propto \epsilon_0^{-1/2}$, our calculated values of k_{14} are likely to be underestimates of the electromechanical coupling coefficients that could be achieved experimentally.

The computed values of ϵ_0, C_{44}, e_{14}, d_{14} and k_{14} are reported in Table I. The values of the piezoelectric constant e_{14} range from 0.01 to 0.81 C/m^2. Seventeen compounds have $e_{14} > 0.16$ C/m^2, the experimentally measured piezoelectric coefficient of GaAs. The highest predicted values are for NiTiSn, PtTiSn and LiGaSi. These three compounds also have the highest values of electromechanical coupling k_{14}, arising from their large e_{14}. LiMgP, LiZnP, and LiZnAs have similarly high k_{14} values, with lower values of e_{14} compensated by lower values of ϵ_0.

It is remarkable that no piezoelectric response data for any half-Heusler compound has yet been reported. With a single-crystal sample of sufficiently low conductivity, the piezoelectric coefficient should be readily measurable for most if not all of these compounds. Moreover, measurements of the dielectric response and elastic coefficients, which also have not been reported to date, would provide an additional test of these theoretical predictions and a more complete characterization of the polarization-related properties of these otherwise much-studied compounds.

Next, we consider the properties of the full set of 987 hypothetical and real ABC combinations identified earlier for study. As before, for each combination we optimize the lattice constant for each of the variants $\underline{A}BC$, $A\underline{B}C$, and $AB\underline{C}$. Choosing the variant having the lowest total energy, we determine whether our LDA calculations predict it to be insulating. Of the 987 combinations, we find 371 insulators having either 8 or 18 valence electrons, while the compounds containing 28 valence electrons are all found to be metallic.

For the insulators, we perform linear-response calculations using ABINIT as described above, except that we also compute the C_{11} and C_{12} elastic constants. This allows us to screen for local elastic stability by requiring that $C_{11}+2C_{12} > 0$, $C_{44} > 0$ and $C_{11}-C_{12} > 0$ [27]. Furthermore, we calculate phonon frequencies at three additional high-symmetry points (X, L and W) and eliminate

ABC	$a_{\text{expt.}}$	a	E_{gap}	e_{14}	d_{14}	C_{44}	k_{14}	ϵ_0
LiMgP	6.02	5.95	1.51	0.32	7.6	0.42	0.15	12
LiMgAs	6.19	6.17	1.55	0.26	6.9	0.37	0.13	12
LiMgBi	6.74	6.71	0.62	0.07	2.8	0.26	0.04	16
LiZnN	4.87	4.77	1.21	0.11	1.3	0.84	0.03	13
LiZnP	5.78	5.59	1.15	0.44	6.6	0.67	0.15	14
LiZnAs	5.94	5.87	1.12	0.43	8.1	0.54	0.16	15
LiCdP	6.09	5.95	0.76	0.14	3.2	0.46	0.05	17
AuScSn	6.42	6.39	0.19	0.17	2.7	0.62	0.05	20
AuYPb	6.73	6.65	0.07	0.44	9.1	0.48	0.13	27
LiGaSi	6.09	5.81	0.08	0.56	8.6	0.65	0.15	22
LiInSi	6.68	6.18	0.07	0.08	1.6	0.51	0.03	23
NiTiSn	5.94	5.89	0.44	0.81	12.9	0.62	0.19	30
NiZrSn	6.11	6.08	0.52	0.19	2.8	0.70	0.05	26
NiHfSn	6.08	6.00	0.41	0.28	3.4	0.80	0.07	24
PdZrSn	6.32	6.27	0.49	0.01	0.1	0.68	0.01	24
PdHfSn	6.30	6.20	0.38	0.06	0.7	0.75	0.01	22
PtTiSn	6.16	6.15	0.82	0.64	9.5	0.67	0.16	25
PtZrSn	6.32	6.32	1.06	0.19	2.5	0.77	0.05	20
PtHfSn	6.31	6.25	0.99	0.23	2.7	0.83	0.06	18
NiScSb	6.06	6.06	0.29	0.15	2.3	0.66	0.04	21
NiScBi	6.19	6.15	0.22	0.20	3.6	0.57	0.06	24
NiYSb	6.31	6.28	0.34	0.20	3.6	0.55	0.06	20
NiYBi	6.41	6.36	0.26	0.14	2.9	0.49	0.05	22
PdScSb	6.31	6.27	0.28	0.03	0.4	0.59	0.01	20
PdYSb	6.53	6.47	0.26	0.23	4.2	0.53	0.08	18
PtScSb	6.31	6.31	0.71	0.07	1.0	0.66	0.02	19
PtYSb	6.54	6.51	0.58	0.19	3.3	0.58	0.06	19

TABLE I. Properties of experimentally synthesized insulating half-Heuslers, grouped by family. Experimental lattice constants (in Å) are from the ICSD. Also presented are the theoretical lattice constant a, band gap E_{gap} (eV), piezoelectric coefficients e_{14} (C/m^2) and d_{14} (pC/N), elastic constant C_{44} (10^{11}Pa), electromechanical coupling coefficient k_{14}, and zero-stress static dielectric constant ϵ_0.

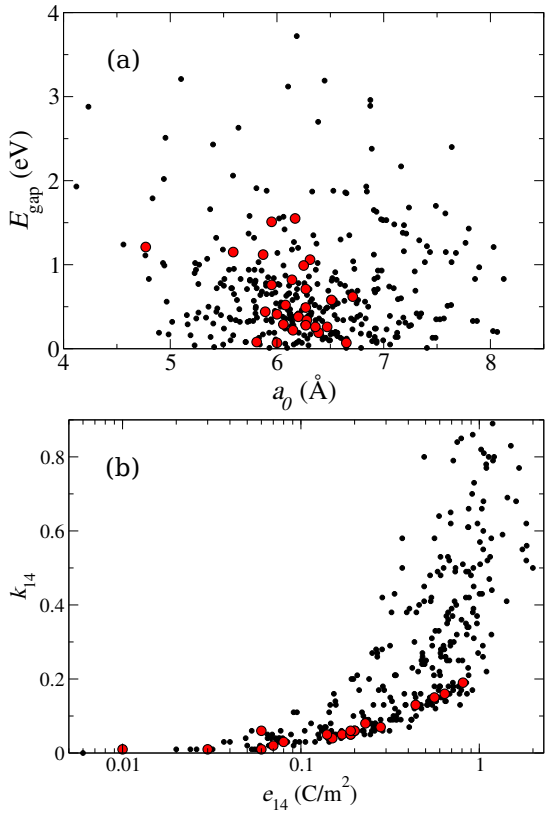

FIG. 2. (Color online) a) Cell parameters (in Å) of insulating ABC combinations as well as their range of band gaps (in eV) are depicted as open black circles. b) Electromechanical coupling factor k_{14} of insulating ABC combinations as a function of piezoelectric constant e_{14}. Known combinations, from Table I, are highlighted as filled red circles.

combinations which exhibit any unstable modes. This reduces the combinations further from 371 down to 312.

We thus arrive at 312 combinations that are predicted to be insulating and locally stable in the lowest-energy variant of the three possible ABC half-Heusler structures. Since DFT tends to underestimate band gaps, we expect that the actual fraction of insulating structures will be slightly higher than our calculations would indicate. The computed band gaps and lattice parameters for these 312 compounds are shown in Fig. 2(a). We expected no particular correlation between lattice parameter and band gap, and indeed we find none. Both quantities are rather broadly distributed, suggesting that there could be considerable flexibility in choosing materials over a substantial range of desired gap or lattice constant.

For these 312 compounds, we compute ϵ_0, C_{44}, e_{14}, d_{14} and k_{14}, using the same methods as before. To give a sense of how the range of properties in the full set of known and hypothetical compounds compares with that of the subset of known compounds, we present a scatter plot of k_{14} vs log e_{14} in Fig. 2(b). It can be seen that there are hypothetical compounds with k_{14} values well above those of known compounds (some have k_{14} close to one). The twenty-seven compounds with the highest values of k_{14} are listed in Table II.

As a guide for experimental investigation of piezoelectric half-Heusler compounds, we highlight a selection of candidate compounds chosen according to relevant practical considerations. We filter the list to eliminate compounds with toxic (Pb, Cd, As) or expensive (Be, Pd, Pt, Au, In) elements. In addition, we require a DFT band gap above 0.4 eV to favor low sample conductivity. Lastly, to promote cation ordering into the lowest-energy variant, we require $\Delta E > 0.15$ eV, where ΔE is the difference in energy between the lowest-energy and next-lowest-energy variants. Those entries in Table II that satisfy these criteria are shown in boldface. Of the 100 compounds that satisfy these criteria, 79 have $e_{14} > 0.16$ C/m^2, the experimentally measured value of GaAs.

Further investigation of the hypothetical half-Heusler piezoelectrics hinges on the possibility of experimentally

ABC	a	$E_{\rm gap}$	e_{14}	d_{14}	C_{44}	k_{14}	ϵ_0
KMgP	6.71	1.04	1.19	346.28	0.03	0.89	13
LiNaS	6.10	3.12	0.92	208.22	0.04	0.86	8
LiSrAs	6.84	1.93	0.79	286.27	0.03	0.85	10
LiNaSe	6.39	2.70	0.75	227.09	0.03	0.84	8
NaMgN	5.43	0.72	1.50	165.23	0.09	0.83	13
NaBeP	5.59	2.06	1.02	192.98	0.05	0.82	11
KMgAs	6.92	0.67	1.06	205.75	0.05	0.81	13
KScPb	7.35	0.42	1.21	330.83	0.04	0.80	25
MgBaSi	7.18	0.37	1.13	290.51	0.04	0.80	21
BeBaSn	6.86	0.16	0.49	1036.54	0.01	0.80	33
KScSn	7.31	0.42	1.19	294.69	0.04	0.79	24
KBeSb	6.51	0.81	0.72	266.50	0.03	0.79	13
MgBaGe	7.21	0.06	1.10	266.49	0.04	0.78	21
AgSrAs	6.72	0.34	1.10	163.79	0.07	0.77	14
NaZnP	6.02	0.76	1.67	163.79	0.14	0.77	16
NaBSi	5.43	0.44	0.94	121.79	0.06	0.73	13
KBaN	6.48	0.69	0.91	174.57	0.05	0.70	18
NaZnAs	6.26	0.16	1.44	98.70	0.15	0.69	18
KYGe	7.13	0.16	1.06	178.85	0.06	0.68	25
CaBAl	5.81	0.37	1.61	99.88	0.16	0.68	21
KMgSb	7.30	0.69	0.87	108.05	0.08	0.66	14
KYSi	7.11	0.14	1.03	167.49	0.06	0.66	25
CuSrAs	6.39	0.36	0.69	179.58	0.04	0.65	19
NaKO	5.90	1.88	0.60	80.78	0.07	0.64	8
KBeBi	6.62	0.34	0.69	127.24	0.05	0.62	16
KAlSi	6.57	0.54	0.98	101.96	0.10	0.62	18
ZnYB	5.78	0.33	1.84	95.35	0.19	0.62	32

TABLE II. Top half-Heusler candidate compounds, ranked according to predicted electromechanical coupling coefficient k_{14}. Those that remain after applying the filtering criteria, as described in the text, are in boldface. Units as in Table 1.

ABC	a	$E_{\rm gap}$	e_{14}	d_{14}	C_{44}	k_{14}	ϵ_0
LiAgTe	6.38	1.02	0.80	28.60	0.28	0.36	17
LiCuTe	6.06	1.57	0.38	8.14	0.38	0.16	14
LiScC	5.23	0.90	0.34	7.73	0.44	0.12	19
LiCuS	5.43	1.32	0.22	4.04	0.55	0.10	10
LiMgSb	6.59	1.30	0.15	4.94	0.30	0.08	14
LiInSi	6.18	0.07	0.08	1.64	0.51	0.03	23

TABLE III. Piezoelectric properties of the previously uncharacterized combinations from Ref. [28] in which the ground state is predicted to be the half-Heusler structure. Units as in Table I.

realizing the desired compounds in the half-Heusler structure. Additional information about bulk equilibrium *ABC* phases can be obtained from the ICSD. In the cases where no phase is reported, it could be that either no stable bulk phase exists with that stoichiometry, or simply that the relevant composition has not been studied. *ABC* combinations are also reported in several structures other than the half-Heusler structure. Specifically, we find that twelve combinations listed in Table II are reported in ICSD with other structures. Nine (KMgP, LiNaS, MgBaSi, MgBeGe, NaZnP, NaZnAs, KMgSb, NaKO, and KMgAs) are reported in the $P4/nmm$ PbClF (also called Cu_2Sb) structure, one (LiNaSe) in the $Pnma$ MgSrSi structure, and two (AgSrAs and CuSrAs) in the $P6_3/mmc$ ZrBeSi structure. One (NaZnAs) is reported in both $P4/nmmm$ and $Fm\bar{3}m$ structures.

First-principles calculations of the total energy of alternative structures can also be used both to predict ground state structures and to identify systems with piezoelectric structures as low-energy alternatives that would be suitable candidates for stabilization through compositional substitution or epitaxial strain. In a recent first-principles study [28] of the stability of ABC compounds, sixteen new combinations are predicted to form in the half-Heusler structure. Of these, fifteen are in our search set, and we find that six are insulating. Our results for these compounds are given in Table III, where the compounds are ranked by k_{14}. It should be noted, however, that 462 of the 987 combinations in our search set were not considered in the stability study; if they had been, the number of compounds in Table III would likely be larger and span a wider range of property values. In any case, absence from this list does not preclude the synthesis of the half-Heusler structure as a metastable phase with appropriate processing. For example, our calculations on KBaN indicate that the half-Heusler structure is the second-lowest in energy among seven structures studied, and is only 0.11 eV higher than the lowest-energy ($Pnma$) structure; such a case could be promising candidate for directed synthesis as a metastable phase.

In summary, we have used a first-principles rational-design approach to demonstrate semiconducting half-Heusler compounds as a previously unrecognized class of piezoelectric materials. We have presented these predictions first for compounds already reported in the half-Heusler structure, and then for a much larger set of candidate combinations that were generated and screened for high performance via a high-throughput analysis. We hope that our results will provide guidance for the experimental realization and further investigation of high-performance materials suitable for practical applications. We also suggest that the combination of piezoelectric properties with other characteristic properties of Heuslers, especially magnetic properties, may offer inviting avenues for further development of multifunctional materials.

Acknowledgments

This work was supported in part by ONR Grant N00014-05-1-0054 and N000-14-09-1-0300. Calculations were carried out at the Center for Piezoelectrics by Design. We thank S.-W. Cheong, C. Felser, K. Garrity, D. R. Hamann, K. Haule, I. Takeuchi, Zhiping Yin and Qibin Zhou for useful discussions.

* These authors contributed equally to this work.

[1] X. Wu, D. Vanderbilt, and D. R. Hamann, Phys. Rev. B **72**, 035105 (2005).
[2] S. Baroni, S. deGironcoli, A. DalCorso, and P. Giannozzi, Rev. Mod. Phys. **73**, 515 (2001).
[3] C. C. Fischer, K. J. Tibbetts, D. Morgan, and G. Ceder, Nature Mater. **5**, 641 (2006).
[4] G. Hautier, C. C. Fischer, A. Jain, T. Mueller, and G. Ceder, Chem. Mater. **22**, 3762 (2010).
[5] H. Nowotny and K. Bachmayer, Monatsch. Chem. **81**, 488 (1950).
[6] A. Belsky, M. Hellenbrandt, V. L. Karen, and P. Luksch, Acta Cryst. **B58**, 364 (2002).
[7] H. C. Kandpal, C. Felser, and R. Seshadri, J. Phys. D. **39**, 776 (2006).
[8] R. A. deGroot, F. M. Mueller, P. G. vanEngen, and K. H. J. Buschow, Phys. Rev. Lett. **50**, 2024 (1983).
[9] S. Chadov, X. Qi, J. Kubler, G. H. Fecher, C. Felser, and S. C. Zhang, Nature Mater. **9**, 541 (2010).
[10] H. Lin, A. Wray, Y. Xia, S. Xu, S. Jia, R. J. Cava, A. Bansil, and M. Z. Hasan, Nature Mater. **9**, 546 (2010).
[11] C. Felser, G. H. Fecher, and B. Balke, Angew. Chem. Int. Ed. **46**, 668 (2007).
[12] Q. Shen, L. Chen, T. Goto, T. Hirai, J. Yang, G. P. Meisner, and C. Uher, Appl. Phys. Lett. **79**, 4165 (2001).
[13] G. S. Nolas, J. Poon, and M. G. Kanatzidis, MRS Bull. **31**, 199 (2006).
[14] B. Balke, J. Barth, M. Schwall, G. H. Fecher, and C. Felser, J. Elec. Mat. **40**, 702 (2011).
[15] S. Ogut and K. M. Rabe, Phys. Rev. B. **51**, 10443 (1995).
[16] D. M. Wood, A. Zunger, and R. deGroot, Phys. Rev. B. **31**, 2570 (1985).
[17] X. Gonze, J.-M. Beuken, R. Caracas, F. Detraux, M. Fuchs, G.-M. Rignanese, L. Sindic, M. Verstraete, G. Zerah, F. Jollet, et al., Comp. Mater. Sci. **25**, 478 (2002).
[18] X. Gonze, G. Rignanese, M. Verstraete, J. Beuken, Y. Pouillon, R. Caracas, F. Jollet, M. Torrent, G. Zerah, M. Mikami, et al., Z. Kristall. **220**, 558 (2005).
[19] X. Gonze, B. Amadon, P. Anglade, J. M. Beuken, F. Bottin, P. Boulanger, F. Bruneval, D. Caliste, R. Caracas, M. Cote, et al., Comp. Phys. Comm. **180**, 2582 (2009).
[20] H. J. Monkhorst and J. D. Pack, Phys. Rev. B **13**, 5188 (1976).
[21] A. M. Rappe, K. M. Rabe, E. Kaxiras, and J. D. Joannopoulos, Phys. Rev. B Rapid Comm. **41**, 1227 (1990).
[22] N. J. Ramer and A. M. Rappe, Phys. Rev. B **59**, 12471 (1999).
[23] http://opium.sourceforge.net.
[24] X. Gonze and C. Lee, Phys. Rev. B **55**, 10355 (1997).
[25] M. Born and K. Huang, *Dynamical Theory of Crystal Lattices* (Oxford University Press, Oxford, 1954), we used Eq. (33.28) from this book.
[26] D. R. Hamann, X. Wu, K. M. Rabe, and D. Vanderbilt, Phys. Rev. B **71**, 035117 (2005).
[27] B. B. Karki, G. J. Ackland, and J. Crain, Journal of Physics: Condensed Matter **9**, 8579 (1997).
[28] X. Zhang, L. Yu, A. Zakutayev, and A. Zunger, Adv. Funct. Mater. **22**, 1425 (2012).